Model-assisted analysis of tomato fruit growth in relation to carbon and water fluxes

Huai Feng Liu, Michel M. Génard, Soraya Guichard, Nadia Bertin

RESEARCH PAPER

Model-assisted analysis of tomato fruit growth in relation to carbon and water fluxes

Huai-Feng Liu[1,2], Michel Génard[1], Soraya Guichard[1] and Nadia Bertin[1,*]

[1] *INRA, UR1115 Plantes et systèmes de culture horticoles, F-84000 Avignon, France*

[2] *Agricultural College, Shi He Zi University, Shi He Zi, Xin Jiang, PR China, 832003*

Abstract

This work proposed a model of tomato growth adapted from the Fishman and Génard model developed to predict carbon and water accumulation in peach fruit. The main adaptations relied on the literature on tomato and mainly concerned: (i) the decrease in cell wall extensibility coefficient during fruit development; (ii) the increase in the membrane reflection coefficient to solute from 0 to 1, which accounted for the switch from symplasmic to apoplasmic phloem unloading, and (iii) the negative influence of the initial fruit weight on the maximum rate of active carbon uptake based on the assumption of higher competition for carbon among cells in large fruits containing more cells. A sensitivity analysis was performed and the model was calibrated and evaluated with satisfaction on 17 experimental datasets obtained under contrasting environmental (temperature, air vapour pressure deficit) and plant (plant fruit load and fruit position) conditions. Then the model was used to analyse the variations in the main fluxes involved in tomato fruit growth and accumulation of carbon in response to virtual carbon and water stresses. The conclusions are that this model, integrating simple biophysical laws, was able to simulate the complex fruit behaviour in response to external or internal factors and thus it may be a powerful tool for managing fruit growth and quality.

Key words: Carbon flux, cell expansion, fruit growth, humidity, *Lycopersicon esculentum*, model, *Solanum lycopersicum*, temperature, tomato, water flux.

Introduction

Size, water, and the content of carbon compounds are the main criteria for assessing the quality for fresh fruits.

Although abundant knowledge is available about the processes involved in growth and primary metabolism, the genetic and environmental improvement of fruit quality remains a complex task due to the antagonism between quality traits, for instance, size and composition. For cultivated tomato, fruit concentration in carbon compounds can be enhanced by cultivation management, but this improvement is often paralleled with an undesirable reduction in yield, mainly due to the decrease of mean fruit size and the increasing incidence of growth disorders (Ho, 2003a). Many studies demonstrated that these effects resulted from alterations in the water and carbon fluxes into the fruit (Ho *et al.*, 1987; Ho and Adams, 1994; Guichard *et al.*, 2001). The development of ecophysiological models of fruit growth seems a good opportunity to manage and optimize fruit quality as they enable us to integrate our understanding of carbon and water fluxes in response to endogenous and external factors (Struik *et al.*, 2005).

Fruit volume increase and accumulation of carbon compounds results from a number of processes such as sugar unloading and metabolism, water import, and cell wall expansion, which are intimately connected at the fruit level and regulated by several steps during fruit development. In their model, Fishman and Génard (1998) proposed an integrative approach of the main processes involved in fruit growth and carbon and water accumulation in peach fruit. This model relies on a biophysical description of water and carbohydrate transport coupled with the stimulation of cell wall extension driven by the influx of water and the turgor pressure (Lockhart, 1965; Zonia and Munnik, 2007). This is a seldom model of fruit growth in which quality is concerned (Bertin *et al.*, 2006). It has been successfully used to analyse the effect of climate fluctuations and orchard management on peach yield and quality (Lescourret and Génard, 2005). Yet no

model of fruit growth coupling carbon and water fluxes has been developed for tomato fruit. Indeed, current tomato models either focus on water import (Bussières, 1994, 2002) or on carbon import (Heuvelink and Bertin, 1994), the dry matter content being empirically deduced. Objectives of this work were to adapt the Fishman and Génard model to tomato fruit in order to predict the influence of environmental conditions on fruit growth in terms of dry and fresh masses.

Tomato fruit growth follows a sigmoid curve and mature fruits contain about 95% of water at maturity. Most of the fruit weight is accumulated during the period of rapid growth which starts about 2 weeks after anthesis and lasts for about 3–5 weeks (Ho and Hewitt, 1986). In tomato, about 80–85% of the water is imported by the phloem tissue (Ho *et al.*, 1987; Guichard *et al.*, 2005) together with carbon which is mainly imported as sucrose. During fruit development, carbon unloading progressively shifts from the symplasmic to the apoplasmic pathway between 15 d and 35 days after anthesis (daa) according to the different authors (Damon *et al.*, 1988; Ruan and Patrick, 1995; Nguyen-Quoc and Foyer, 2001; Ho, 2003*b*). Fruits from most of the cultivated cultivars accumulate mainly fructose and glucose and, to a lesser extent, sucrose. The tomato fruit osmotic pressure is stable throughout fruit development (Ho *et al.*, 1987; Mitchell *et al.*, 1991). Under non-stressed conditions, hexoses, inorganic ions, and organic acids account for, respectively, about 52%, 32%, and 16% of total fruit osmotic potential (Mitchell *et al.*, 1991).

In the following sections, the main equations of the Fishman and Génard model, which drive the water and carbon accumulation during fruit development and the modifications made according to the abundant literature on the regulation of tomato fruit growth are presented. The model was then calibrated on 17 experimental data-sets obtained under fluctuating conditions on the same

tomato cultivar. A cross validation of the model and a sensitivity analysis were performed. Finally, the model could be applied to analyse the effect of virtual carbon and water stresses on the main fluxes involved in fruit growth and the accumulation of carbon compounds.

Model presentation

In the Fishman and Génard model (1998), the fruit is assimilated to one big cell separated from the exterior (xylem or phloem tissue) by a composite membrane. The variations in fruit fresh and dry masses are determined by carbon and water flows across this membrane, which are described by thermodynamic equations involving the hydraulic conductivity of the membrane, the differences in hydraulic and osmotic pressures on both sides of it, and the impermeability of the membrane to solutes. The simulation mainly covers the period of rapid fruit growth, and thus starts about 10 daa, as cell proliferation almost ceased. Input variables are the temperature and air humidity, stem water potential, and phloem sugar concentration. In the following section, only the main equations governing fruit growth or those which were changed to account for tomato specificities are described. Model parameters fitted from the literature on tomato are listed in Table 1.

The temporal variations in fruit fresh mass (w, g) and dry mass (s, g) result from the balance between in and out flows:

$$\frac{dw}{dt} = U_{\mathrm{x}} + U_{\mathrm{p}} - T_{\mathrm{f}} \qquad (1)$$

where U_{x} and U_{p} are the xylem and phloem water inflows (g h^{-1}) and T_{f} is the fruit transpiration outflow (g h^{-1}), which depends on the fruit area A_{f} (cm^2), on the permeation coefficient (ρ, g cm^{-2} h^{-1} MPa^{-1}) of the fruit surface to water vapour, and on air temperature and humidity. A_{f} was

Table 1. *List of parameters estimated from literature data and input in the tomato model*

Parameter	Symbol and value	Unit	Reference (species)
Growth respiration coefficient	$q_{\mathrm{g}} = 0.22$	–	Gary *et al.*, 1998 (tomato fruit)
Maintenance respiration coefficient	$q_{\mathrm{m}} = 0.00042$	g CH$_2$O g^{-1} DM h^{-1}	Bertin and Heuvelink, 1993 (tomato fruit)
Effect of T °C on q_{m}	$Q_{10} = 1.4$	–	Bertin and Heuvelink, 1993 (tomato fruit)
Permeation coefficient of fruit surface to water vapour	$\rho = 0.162$	g cm^{-2} h^{-1} MPa^{-1}	Leonardi *et al.*, 1999 (tomato fruit)
Phloem hydraulic conductivity for water	$L_p = 0.15$	g cm^{-2} MPa^{-1} h^{-1}	Maggio and Joly, 1995; Zwieniecki and Boersma, 1997 (tomato root; mean value)
Michaelis constant for active transport of sugar	$K_{\mathrm{m}} = 0.08$		Milner *et al.*, 1995 (tomato tonoplast sucrose transport)
Proportion of soluble sugars in fruit dry matter	$Z = 0.52$	g g^{-1}	S Guichard unpublished data (tomato fruit)
Membrane permeability for sugar diffusion	$P_{\mathrm{s}} = 3.6 \times 10^{-5}$	g cm^{-2} h^{-1}	Ruan and Patrick, 1995 (tomato pericarp phloem membrane)
Threshold hydrostatic pressure for cell growth	$Y = 0.1$	MPa	Grange, 1995 (tomato pericarp)
Cell wall extensibility	$\Phi_{\max} = 0.2$	MPa^{-1} h^{-1}	Cosgrove, 1985 (pea stem)
Water density	$D_{\mathrm{w}} = 1$	g cm^{-3}	

deduced from tomato fresh weight (W_f) by the empirical equation $A_f = 5.9436 W_f^{0.6641}$ experimentally determined.

$$\frac{ds}{dt} = U_s - R_f \tag{2}$$

where U_s is the phloem sugar input (g h^{-1}) and R_f is the fruit respiration rate (g h^{-1}). R_f is the sum of (i) growth respiration which is proportional to the growth respiration coefficient (q_g) and to the dry mass increment, and (ii) maintenance respiration which is proportional to the maintenance coefficient (q_m) and to the fruit dry mass and depends on temperature through a Q_{10} parameter.

U_x and U_p are calculated from non-equilibrium thermodynamic equations as:

$$U_x = A_x L_x \left[P_x - P_f - \sigma_x (\pi_x - \pi_f) \right] \tag{3}$$

$$U_p = A_p L_p \left[P_p - P_f - \sigma_p (\pi_p - \pi_f) \right] \tag{4}$$

where subscripts x, p, and f refer to xylem, phloem, and fruit, respectively. A_x and A_p, the surface (cm^2) of exchange between the vascular networks entering the fruit and the fruit compartment, are assumed to be proportional to the fruit surface area (A_f) according to a constant non-dimensional coefficient a ($A_x = A_p = aA_f$). L_x and L_p are hydraulic conductivity (g cm^{-2} MPa^{-1} h^{-1}), σ_x and σ_p are solute reflection coefficients of the membrane separating the fruit from the conducting tissues. P and π are the hydrostatic and osmotic pressures (MPa). As first approximations, $\sigma_x = 1$ and $\pi_x = 0$ (Fishman and Génard, 1998). The fruit and phloem osmotic pressures are calculated from the molar concentrations of osmotically active compounds according to Nobel (1974). It was assumed that a constant proportion Z of accumulated sugars remains in soluble forms, thus contributing to the osmotic pressure, whereas the rest was converted into structural material. The contribution to the fruit osmotic potential of osmotically active substances other than carbohydrates (such as amino acids, inorganic ions. and organic acids) was assumed to be constant during fruit development (Ho *et al*., 1987; Mitchell *et al*., 1991). This contribution was calculated at the initial stage (10 daa) as equal to the contribution of soluble sugars.

In equation 4, the reflection coefficient σ_p varies from 0 (fully permeable membrane, for instance for symplasmic pathway) to 1 (fully impermeable membrane, for instance in the absence of symplasmic connection). It accounts for the different pathways of sugar transport from the phloem to the sink cells, and it was considered as constant in the original model. As in grape berry (Zhang *et al*., 2006), the transport of sugar into the sink cells of tomato fruit progressively shifts from the symplasmic to the apoplasmic pathway during fruit development (Damon *et al*., 1988; Ruan and Patrick, 1995; Brown *et al*., 1997). This shift of phloem sugar unloading from the symplasmic to

the apoplasmic pathway was represented by a gradual temporal increase of σ_p empirically expressed as:

$$\sigma_p = 1 - \exp(-\tau \times t^2) \tag{5}$$

where t is simulation time in hours ($t=0$ corresponds to 10-d-old fruits), and τ a constant parameter.

Now as detailed in the original model, carbohydrates can be transported from the phloem to the fruit by active transport (U_a), by mass flow and by passive diffusion across the membrane:

$$U_s = \overbrace{\frac{s \times v_m \times C_p}{\{(K_M + C_p) \times (t + \delta \times s_0^f)\}}}^{\text{Active transport}}$$
$$+ \overbrace{(1 - \sigma_p) C_s U_p}^{\text{Mass flow}} + \overbrace{A_p p_s (C_p - C_f)}^{\text{Passive diffusion}} \tag{6}$$

where v_m is a kinetic constant (g sucrose g^{-1} DW h^{-1}), K_m is the Michaelis constant, C_p and C_f are the sugar concentrations in the phloem and in the fruit, respectively (g g^{-1}), C_s is the mean of these two concentrations, and p_s is the solute permeability coefficient (g cm^{-2} h^{-1}). The second term of the denominator of U_a accounts for an inhibitory effect which increases with fruit age or time (t, hour). In the original model this inhibitory effect exponentially increased with time after a given developmental stage. In the case of tomato, this inhibitory effect was linked to the initial dry weight of the fruit s_0 through two parameters δ and f. Indeed, as the weight of young tomato fruits is positively correlated with the number of cells (Bertin *et al*., 2003a), the competition for carbon among individual cells may be higher in large fruit as suggested by previous studies (Bertin, 2005), which may reduce the uptake of carbon by each individual cell. As defined here, the maximum uptake rate of sucrose decreased with fruit age:

$$V_{\max} = \frac{v_m}{t + \delta \times s_0^f}$$

These equations representing the different fluxes involved in water and carbon balance in the fruit could be combined as follows with the Lockart (1965) equation relating the variations in fruit/cell volume (dV/dt) to the hydrostatic pressure P_f, to the threshold value Y (MPa) above which irreversible extension occurs, and to the cell wall extensibility (Φ MPa^{-1} h^{-1}):

$$\frac{dV}{dt} = V\Phi(P_f - Y) = \frac{U_x + U_p - T_f}{D_w} + \frac{U_s - R_f}{D_s} \tag{7}$$

where D_w and D_s are, respectively, the water and sugar densities (g cm^{-3}), and $P_f \geq Y$. In a first approximation the second term of the right side in equation 7 is relatively

small and may be neglected. Whereas Φ was constant in the original model, it was assumed here, as for mango fruit (Lechaudel *et al.*, 2007), that the cell wall extensibility exponentially decreased during tomato fruit growth according to two parameters Φ_{max} and k:

$$\Phi = \frac{\Phi_{max}}{1 + \exp(kt)} \tag{8}$$

This decrease is consistent with the decreasing activity observed in tomato epidermis and pericarp of xyloglucan-specific enzymes (Thompson *et al.*, 1998) involved in the mechanical changes underlying cell-wall mechanical properties and growth processes (Thompson, 2001; Cosgrove, 1993). Moreover, the extensive cutinization of epidermal cell wall and thickening of the cuticle during ripening of tomato fruit (Bargel and Neinhuis, 2005) may also contribute to the decline of Φ.

Finally, the hydrostatic pressure P_f could be deduced from equation 7 as a function of other variables. Assuming that xylem and phloem water potentials are equal to the stem water potential Ψ_w, it becomes possible, by combining the different equations, to calculate the sugar and water fluxes in the fruit and to integrate them over time. The diurnal course of the stem water potential in greenhouse tomato presents maximum values around -0.05 MPa at predawn and minimum values in the afternoon depending on air *VPD* (Guichard *et al.*, 2005). An experimental regression between air *VPD* (kPa) and stem water potential (MPa) established on different days in two greenhouse compartments at low and high air *VPD* (S Guichard, unpublished data) was applied in the model:

$$\Psi_W = \Psi_X - \Psi_p = -0.1922VPD^{0.5105} \tag{9}$$

Px and Pp (equations 3 and 4) could then be calculated from the Nobel (1974) equation $\Psi = P - \pi$, assuming $\sigma_x = 1$ and $\pi_x = 0$, and calculating π_p from the phloem sap concentration in sugars.

Model parameterization

Model parameters were either estimated from experimental data as described in the Materials and methods, or taken from the literature. The latter were almost all specific for tomato fruit (Table 1). The xylem hydraulic conductivity (L_x) was assumed to be proportional to the phloem conductivity (L_p): $L_x = 0.22L_p$, on the basis of known proportions of water transported by xylem and phloem tissues (18% and 82%, respectively) (Ho *et al.*, 1987; Plaut *et al.*, 2004; Guichard *et al.*, 2005). The phloem sucrose concentration (C_p, equation 6) was assumed to be constant. It was independently calculated on the 17 datasets from the increase in fruit dry and fresh weights, and from the amounts of sugar and water lost by respiration and transpiration, respectively (parameters

given in Table 1). Considering that the phloem flux accounts for 85% of the total water influx, then the sucrose concentration of the phloem sap was estimated as the ratio between sugar and water amounts imported by the phloem tissue. A mean value of 0.11 g g^{-1} was found which is fairly consistent with the range of values reported for tomato in the literature. Ho *et al.* (1987) estimated that the phloem sap concentration decreased during fruit development, from 7.1% to 2.9% dry matter at a salinity of 2 mS cm^{-1} and from 12.5% to 7.8% at a salinity of 17 mS cm^{-1}. Plaut *et al.* (2004) found a phloem sap concentration in organic compounds ranging from 5% to 8% which was rather stable during fruit development.

Six other parameters were estimated by fitting the simulated curves of fresh and dry weight increases to the experimental curves: τ involved in the shift from symplasmic to apoplasmic carbon unloading (equation 5), v_m, δ, and f intervening in the active transport of carbon (equation 6), k determining the cell wall extensibility fluctuations during fruit development (equation 8) and $a = A_x/A_f = A_p/A_f$ the ratio between the surface of vascular networks and the fruit area (equations 3 and 4).

Materials and methods

Experimental conditions

Seventeen datasets were collected from three experiments performed at INRA Avignon (south of France) in 1998, 2000, and 2001 with the same tomato cultivar (*Lycopersicon esculentum* Mill. cv. 'Raïssa'). The 1998 experiments were conducted from spring to summer in two greenhouse compartments under high (*VPD*+) or low (*VPD*–) air vapour pressure deficit (*VPD*). For each humidity regime, inflorescences were pruned either to three flowers (3F) or to six flowers (6F) (detailed in Guichard *et al.*, 2005). Fruit growth parameters were measured once in spring and once in summer, so that this experiment represented eight datasets. In 2000, the experiment was carried out in growth climatic chambers under three controlled day/night air temperature regimes: 20/20 °C, 25/25 °C or 25/20 °C. A 12 h photoperiod was applied at a photosynthetic photon flux density of about 500 μmol m^{-2} s^{-1}*PAR* above the canopy. For each temperature regime, inflorescences were pruned to two (2F) or five (5F) fruits (detailed in Bertin, 2005). The 2001 experiment was carried out in a growth chamber with a controlled day/night air temperature of 25/20 °C and a 12 h photoperiod at a light intensity of about 500 μmol m^{-2} s^{-1}*PAR* above the canopy (detailed in Bertin *et al.*, 2003b). The first truss was pruned to six flowers (6F) and the second truss was pruned to two flowers (2F). Plants were stopped two leaves above the second truss.

The fruit position influence was considered in the 2000-5F and 2001 experiments. Within the inflorescence, fruits were classified as proximal (first and second fruits: F1F2), median (third and fourth fruits: F3F4), and tip (fifth and sixth fruits: F5F6) fruits. Air temperature and humidity were recorded hourly in each experiment and input in the model as external signals. The 17 datasets and corresponding experimental conditions are summed up in Table 2. Tomato fruit diameter, fresh weight, and dry weight were measured weekly in the 1998 experiment and every 2–5 d in the 2000 and 2001 experiments. The 10 daa (start of simulation) dry and fresh weights were estimated by exponential interpolation considering the experimental data from 7 daa to 14 daa.

Table 2. *Mean environmental conditions and mean fruit dry and fresh masses at 10 d after anthesis (initial weights for the model)*

Treatment names indicate climatic treatments (high or low air vapour pressure deficit: *VPD+* and *VPD–*; day/night air temperature °C, inflorescence size (2F, 3F, 5F or 6F) and fruit position within the inflorescence when it was considered (F1 to F6). In the 1998 experiments fruits were sampled for measurements once in spring and once in summer. 1998 experiments took place in greenhouse, whereas 2000 and 2001 experiments were performed in growth chambers.

Experiment	Treatments	Day/night temperature (°C)	Day/night humidity (%)	Day/night VPD (kPa)	10 daa dry mass (g)	10 daa fresh mass (g)
1998	VPD+3Fspring	26/19	47/70	1.8/0.7	0.47	6.14
1998	VPD+6Fspring				0.3	3.84
1998	VPD-3Fspring	25/18	62/73	1.2/0.6	0.35	5
1998	VPD-6Fspring				0.21	2.14
1998	VPD+3Fsummer	28/21	49/75	1.9/0.6	0.46	6.61
1998	VPD+6Fsummer				0.2	2.47
1998	VPD–3Fsummer	27/20	62/77	1.3/0.6	0.63	6.94
1998	VPD–6Fsummer				0.19	1.46
2000	20°C-2F	20/20	70	0.7	0.37	4.97
2000	25°C-2F	25/25		0.9	1.23	16.76
2000	2520°C-2F	25/20		0.9/0.7	0.77	10.38
2000	2520°C-5F-F1	25/20	70	0.9/0.7	0.75	9.73
2000	2520°C-5F-F3				0.55	7.62
2000	2520°C-5F-F5				0.22	12.74
2001	2520°C-6F-F1F2	25/20	75	0.8/0.6	0.53	6.3
2001	2520°C-6F-F3F4				0.47	5.9
2001	2520°C-6F-F5F6				0.4	4.62
	Average				0.48	6.1

Goodness-of-fit and predictive quality of the model

Model solving and calibration were performed using R language (R Development Core Team, 2005). Fresh and dry matter growth curves were fitted by minimizing the weighed (variance) mean squared error using the Nonlinear Least Squares Regression function. The goodness of fit of the model was evaluated through the relative root mean squared error (*RRMSE*) (Kobayashi and Us Salam, 2000), which is a common criterion to quantify the mean difference between simulation and measurement:

$$RRMSE = \frac{1}{\bar{y}} \sqrt{\frac{\sum_{i=1}^{N} n_i (y_{imod} - \bar{y}_{idata})^2}{\sum_{i=1}^{N} n_i}} \qquad (10)$$

where *N* is the number of sample dates over the fruit growth period, n_i is the number of repetitions at date *i*, y_{imod} is the fruit dry or fresh mass calculated by the model at date *i*, $\bar{y}_{idata}$ is the mean value measured at date *i*, and $\bar{y}$ is the mean of all measured values. The smaller the *RRMSE* in comparison to measurements, the better is the goodness-of-fit.

The predictive quality of the model, which evaluates the validity of the model over a range of datasets, was calculated with a cross validation approach (Thorp *et al*., 2005) by splitting the 17 experimental datasets into eight situations, i.e. spring *VPD+* data, spring *VPD–* data, summer *VPD+* data, summer *VPD–* data, 20/20 °C data, 25/20 °C data, 25/25 °C data, and 2001 year data. The cross validation requires eight successive calibrations of the model by alternatively leaving out one situation or dataset. Then the model was evaluated using the fitted parameters to simulate the left out dataset. The criterion was the relative root mean squared error of prediction (*RRMSEP*). Averaging the *RRMSEP* over all the situations gives the overall estimation of the prediction error.

Sensitivity analysis

A sensitivity analysis was performed to identify the most influential factors on the model response. The investigated factors were temperature, humidity, phloem sugar concentration, stem water potential, initial fruit dry mass (s_0), and fresh mass (w_0). The values tested for these factors are in the range of those experimentally observed or reported in literature (Table 3). For the initial weights, it was considered that the percentage of dry matter was constant (7.5%) and thus only pairwise variations of s_0 and w_0 were tested. The sensitivity of the model to the given variation of one factor was quantified by the normalized sensitivity coefficient, defined as the ratio between the variation of fruit dry or fresh mass at the end of the simulation (ΔW) relative to its average value ($\bar{W}$) and the variation of the input values for the factor (ΔP) relative to its average value ($\bar{P}$). Sensitivity coefficients were calculated for each individual factor considering stepwise increases of this factor (as defined in Table 3), all other factors being at standard values:

$$\text{sensitivity coeff.} = \frac{\Delta W / \bar{W}}{\Delta P / \bar{P}} \qquad (11)$$

Then the mean normalized sensitivity coefficients for the fresh and dry weights were calculated over the whole range of variation for each factor.

Results

Global estimation of parameters, goodness-of-fit, and predictive quality of the model

The average dry mass (s_0) and fresh mass (w_0) of 10 daa fruits were input as the initial values of simulation for each dataset (Table 2). The six parameters mentioned above were globally estimated on the 17 experimental datasets:

$$v_m = 3.53 \text{ g sucrose g}^{-1} \text{ dm h}^{-1}, \delta = 1170,$$

$$f = 0.45, a = 0.011, k = 0.0066, \tau = 3.3810^{-6}$$

Dynamics of V_{max}, σ_p, and Φ are depicted in Fig. 1. The reflection coefficient σ_p showed a sigmoid evolution and

Table 3. *Range of values for the different factors considered in the model sensitivity analysis*

Temperature (°C)	Relative humidity (%)	Phloem Sugar concentration (g g^{-1})	Stem water potential (MPa)	Initial dry mass (g)	Initial water mass (g)
15	50	0.04	−0.36	0.1	1.3
20	60	0.08	−0.29	0.5	6.7
25	70	0.12	−0.22	1.0	13
30	80	0.16	−0.15	1.5	20
35	90	0.20	−0.08	2.0	27

the apoplasmic sugar unloading went up at about 11 daa (σ_p >0). The cell wall extensibility sharply decreased during the first 15 d of simulation and reached zero around 45 daa. The maximum rate of carbon uptake (V_{max}) exhibited a 2–3-fold decrease over the growth period, depending on s_0 which mainly affected the initial V_{max}; the initial value of V_{max} increased from 0.0028 to 0.0042 and 0.0062 g sucrose g^{-1} DW h^{-1} when s_0 decreased from 1.23 to 0.48 and 0.20 g. At fruit maturity (about 60 daa), V_{max} ranged between 0.0014 and 0.0020 g sucrose g^{-1} DW h^{-1}.

The model simulations obtained with the global set of parameters were applied to experimental measurements of dry and fresh masses for each experiment (Figs 2, 3, 4) and *RRMSE* are given in Table 4. The mean *RRMSE* was 0.23 for the fruit dry mass and 0.25 for the fruit fresh mass. The goodness-of-fit was satisfying for the 1998 experiment both in dry (0.03 to 0.22) and fresh masses (0.05 to 0.30), and it was on average lower (higher *RRMSE*) for the 2000 and 2001 datasets (0.23 to 0.59 for dry weight and 0.24 to 0.55 for fresh weight). In spring (Fig. 2) the model accurately simulated fruit growth on the 6F-plants despite a slight underestimation of the fresh weight at high *VPD*, but underestimated the fresh and dry weights on the 3F-plants at both low and high *VPD*. In summer, the simulations adequately fitted the experimental growth curves on both 3F- and 6F-plants at low *VPD*, but at high *VPD* under stressed conditions the dry weight was slightly underestimated by the model for both 3F- and 6F-plants. The 2000 dataset comparing 2-F plants at three temperature regimes (Fig. 3) was well simulated by the model except an underestimation at 20 °C. At this temperature the growth rate was reduced, but the final fruit size was not affected due to a longer period of growth. The fruit position effect was considered in the 2000 and 2001 datasets (Fig. 4). The reduction in fruit growth at the tip position within the inflorescence was accurately simulated by the model until about 35 daa, so that the final fresh and dry weights were underestimated.
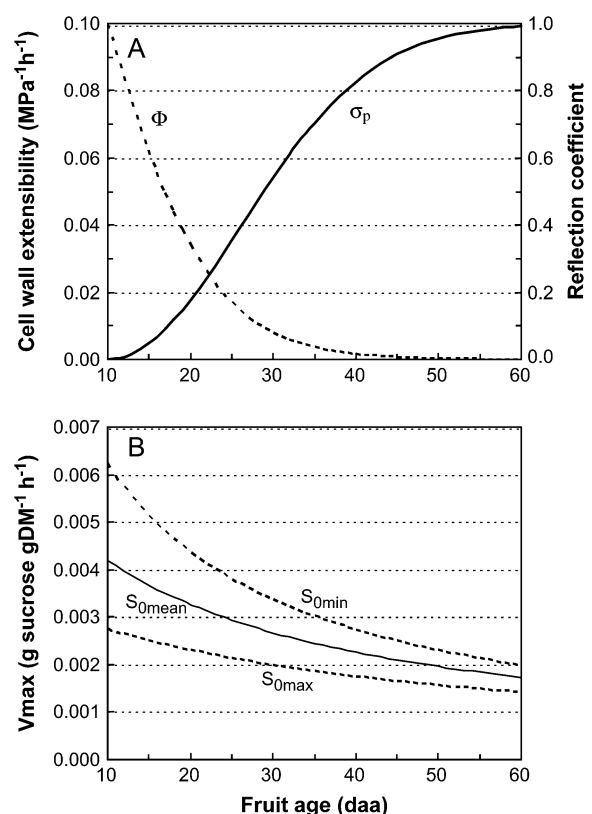

Fig. 1. Temporal dynamics of (A) the solute reflection coefficient for phloem unloading σ_p (equation 5), the cell wall extensibility Φ (equation 8), and (B) the maximum rate of carbon uptake from phloem $V_{max} = \frac{v_m}{t + \delta \times s^r_0}$ (equation 6) for three values of the 10 daa fruit dry weight ($s_{0max}=1.23$ g, $s_{0mean}=0.48$ g, and $s_{0min}=0.20$ g which are the maximum, average, and minimum values experimentally observed; Table 2).

The cross validation allowed the predictive quality of the model to be evaluated in the different situations. *RRMSEP* values ranged from 0.02 to 0.76 for the dry weight (mean value=0.27) and from 0.04 to 0.72 for the fresh weight (mean value=0.30). The 1998 experiments were better predicted by the model, whereas the tip fruit
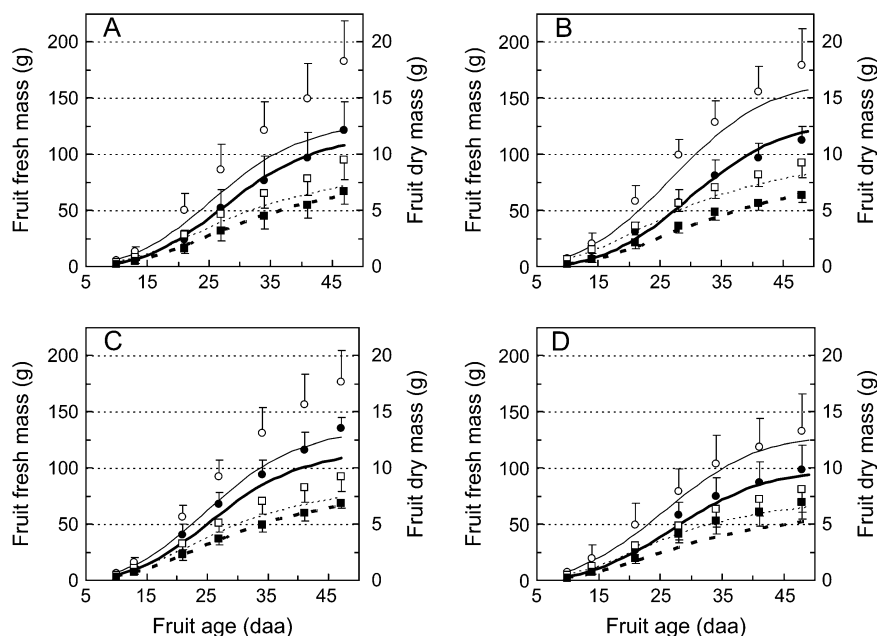
Fig. 2. Dynamics of measured (symbols) and simulated (lines) fruit fresh (circles, solid line) and dry (squares, dotted line) weight during fruit ageing for the *VPD* and fruit load treatment detailed in Table 2. (A) VDP-3Fspring (open symbols, thin line) and VPD-6Fspring (closed symbols, bold line); (B) VDP-3Fsummer (open symbols, thin line) and VPD-6Fsummer (closed symbols, bold line); (C) VDP+3Fspring (open symbols, thin line) and VPD+6Fspring (closed symbols, bold line); (D) VDP+3Fsummer (open symbols, thin line) and VPD+6Fsummer (closed symbols, bold line). Simulations started 10 daa. Each point is an average of 5–10 measurements and vertical bars indicate standard deviations.

positions in the 2000 dataset were predicted less accurately, but the high *RRMSEP* may be due to high scattering of this dataset.

Sensitivity analysis of the model

To understand the response of the model to fluctuations of the fruit environment, a sensitivity analysis to temperature, humidity, stem water potential, phloem sugar concentration, and initial fruit dry and fresh weights was performed. The mean normalized sensivity coefficients for the fresh and dry fruit weight and their range of variation are shown in Fig. 5. The model was mainly sensitive to the phloem sucrose concentration (C_p) involved in the control of fruit sugar import (equation 6). Concerning the fruit dry weight, the model sensitivity to the initial weight, to temperature and to stem water potential was low and in the same range (0.19 to 0.26 in absolute values), whereas the sensitivity to humidity was almost nil. Concerning the fresh weight, the model was hardly sensitive to temperature, and moderately sensitive to the initial dry or fresh weight, to stem water potential and to humidity (0.21 to 0.39). The model sensitivity to a given factor went up as this factor increased in the range described in Table 3, except for the stem water potential (Fig. 5). The largest range of variation concerned the sensitivity to C_p.

The model sensitivity to interactions between C_p and other factors is shown in Fig. 6 for the highest sensitivity

coefficients. As C_p increased from 0.04 to 0.20 g sucrose g^{-1}, the sensitivity of the model to C_p increased 2–3-fold for the dry and fresh weights, respectively. No additive effects and only very small interactions among variables or parameters were observed except a slight additive interaction between C_p and initial weights. Indeed for both fresh and dry weights, the model sensitivity to C_p decreased 1.9-fold at a low C_p value and 1.5-fold at a high C_p value as the initial weights increased. For other variables, only small interactions could be observed (for instance between humidity and temperature, or between stem water potential and initial weights) and in very low ranges of sensitivity (not shown).

Analysis of main components of fruit growth under situations of carbon and water stresses

Responses of the main fluxes and factors involved in the control of fruit growth (phloem and xylem fluxes, transpiration and respiration rates, carbon transport pathways, osmotic and turgor pressures) to given variations in C_p, in air temperature and humidity, and in stem water potential were analysed with the model. Carbon stress was virtually applied by reducing the phloem carbon concentration (C_p) from 0.12 to 0.06 g g^{-1}. Water stress was simulated first by decreasing the stem water potential from –0.22 to –0.6 MPa at constant air humidity (70%), and then by decreasing the air humidity from 70% to 40% at constant stem water potential (–0.22 MPa). All other
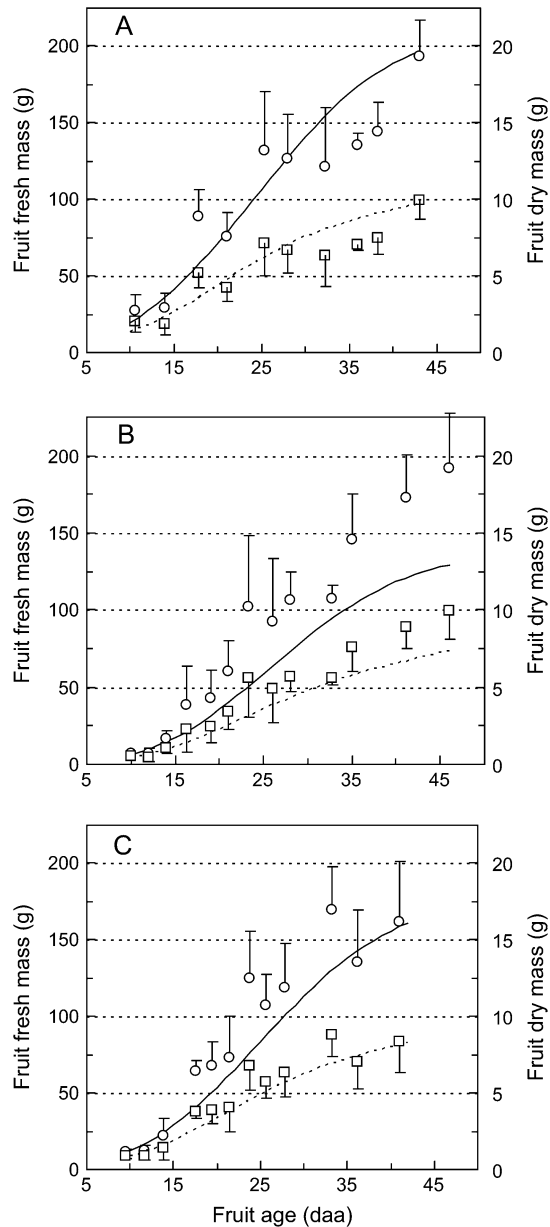
Fig. 3. Dynamics of measured (symbols) and simulated (lines) fruit fresh (circles, solid line) and dry (squares, dotted line) weight during fruit ageing for the temperature treatment at low fruit load detailed in Table 2. (A) 25°C-2F treatment; (B) 20°C-2F treatment; (C) 2025°C-2F treatment. Simulations started 10 daa. Each point is an average of 5–10 measurements and vertical bars indicate standard deviations.
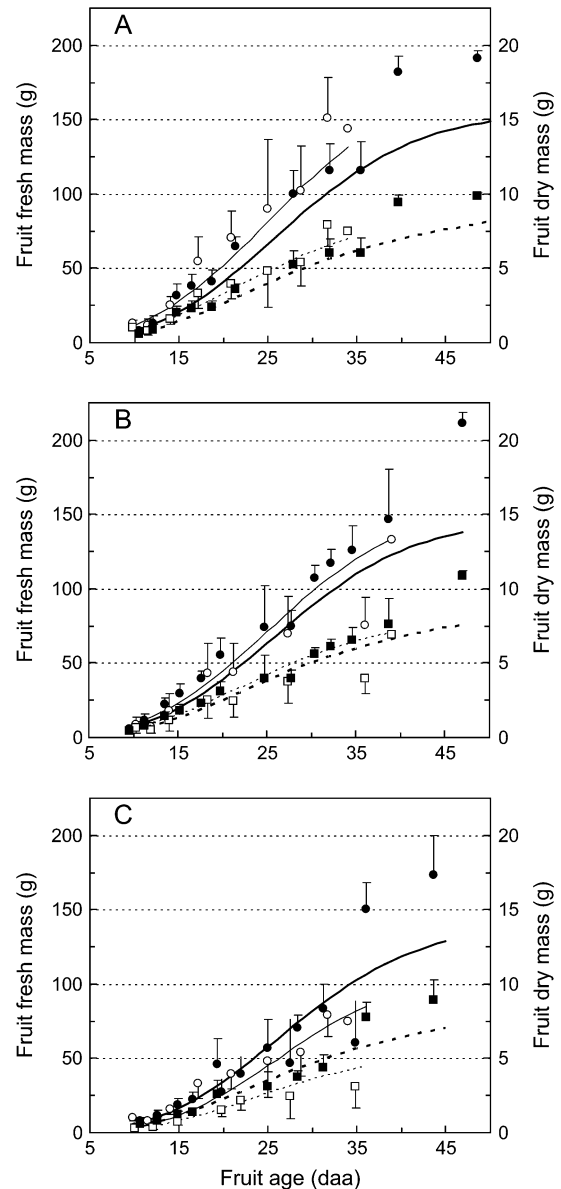

Fig. 4. Dynamics of measured (symbols) and simulated (lines) fruit fresh (circles, solid line) and dry (squares, dotted line) weight during fruit ageing for the fruit position effect detailed in Table 2. (A) 2520°C-5F-F1 treatment (open symbols, thin line) and 2520°C-6F-F1F2 treatment (closed symbols, bold line); (B) 2520°C-5F-F3 treatment (open symbols, thin line) and 2520°C-6F-F3F4 treatment (closed symbols, bold line); (C) 2520°C-5F-F5 treatment (open symbols, thin line) and 2520°C-6F-F5F6 treatment (closed symbols, bold line). Simulations started 10 daa. Each point is an average of 5–10 measurements and vertical bars indicate standard deviations.

model parameters were those globally estimated on the 17 experimental datasets.

The carbon stress induced a decrease in the final dry and fresh weights of, respectively, 71% and 51%. This response was related to a decrease of all fluxes: both xylem and phloem water influx decreased by about 50%, whereas the respiration and transpiration rates dropped by, respectively, 68% and 31% over the growth period compared with the standard conditions. The reduction of C_p directly decreased the active transport of carbon

(equation 6) and thus the accumulation of carbon compounds in the fruit, resulting in a drop and then in the stabilization of the fruit osmotic potential π_f (–16% on average over the growth period). The consequent reduction of xylem and phloem fluxes induced a decrease of the fruit turgor pressure (–16% on average over the period), which then resulted in a lowered volume or fresh

Table 4. *Goodness-of-fit (*RRMSE*) and quality of prediction (*RRMSEP*) of the model for tomato fruit dry (DM) and fresh (FM) masses*

Treament	*RRMSE* DM	*RRMSE* FM	*RRMSEP* DM	*RRMSEP* FM
VPD+3Fspring	0.21	0.28	0.17	0.25
VPD+6Fspring	0.03	0.17	0.02	0.14
VPD-3Fspring	0.22	0.30	0.09	0.19
VPD-6Fspring	0.03	0.06	0.25	0.36
VPD+3Fsummer	0.10	0.07	0.05	0.04
VPD+6Fsummer	0.14	0.05	0.12	0.05
VPD-3Fsummer	0.12	0.14	0.07	0.11
VPD-6Fsummer	0.07	0.06	0.32	0.72
20°C-2F	0.32	0.39	0.33	0.40
25°C-2F	0.23	0.24	0.35	0.37
2025°C-2F	0.25	0.29	0.30	0.31
2025°C-5F-F1	0.23	0.25	0.26	0.27
2025°C-5F-F3	0.58	0.55	0.67	0.60
2025°C-5F-F5	0.59	0.48	0.76	0.56
2025°C-6F-F1F2	0.24	0.25	0.23	0.23
2025°C-6F-F3F4	0.23	0.31	0.19	0.26
2025°C-6F-F5F6	0.31	0.31	0.33	0.28
Mean	0.23	0.25	0.27	0.30
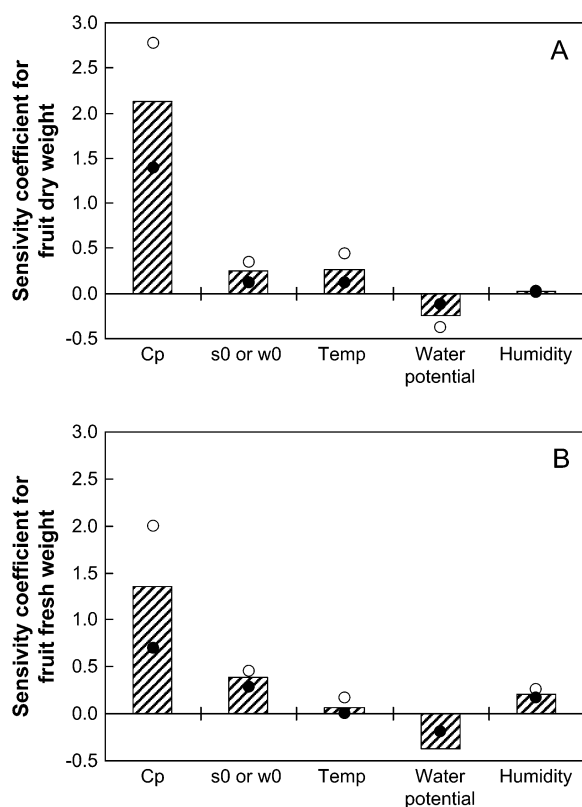
Fig. 5. Mean normalized sensivity coefficients (bars) calculated for the dry (A) and fresh (B) weights according to given variations in phloem sucrose concentration (C_p), initial dry and fresh weights (s_0 and w_0), air temperature, stem water potential, and air humidity. Circles indicate the range of variation of each coefficient calculated for the minimum (closed circles) and maximum (open circles) value of each factor (see Table 3).

weight increase. The mass flow transport of carbon was also reduced, especially at the beginning of the growth period (not shown) due to the reduction of the phloem influx. At the end of the simulation period the final fruit dry matter content was reduced by 41% (3.69 against 6.24% in standard conditions).

Low air humidity affected only the fruit fresh weight (–9%) through a 2-fold higher transpiration rate. This loss of water concentrated the fruit carbon compounds and increased the fruit osmotic pressure. For this reason the xylem and, to a lesser extent, the phloem water imports were slightly increased during the second period of simulation. However, this could not compensate for the loss of water by transpiration. Finally, the fruit dry matter content was increased by 8% (6.77% against 6.24% in standard conditions).

Reducing the stem water potential from –0.22 MPa to –0.6 MPa reduced the final fresh and dry fruit weight by, respectively, 44% and 29% compared with the standard situation. This firstly resulted from the reduction of the xylem-to-fruit and phloem-to-fruit gradient of water potential, which lessened the xylem and phloem water imports by, respectively, 67% and 48% over the simulation period. Transpiration and respiration rates were reduced by, respectively, 35% and 31% over the growth period. Due to the lower influx of water, the fruit osmotic pressure was increased by 31% over the growth period which only very slightly compensated for the drop of xylem and phloem fluxes, and indeed the fruit turgor pressure was reduced by 22% over the growth period. The final fruit dry matter content was increased by 27% (7.89% against 6.24% in standard conditions). The relative proportions of the different pathways of carbon transport were affected, neither by air humidity nor by stem water potential (not shown).
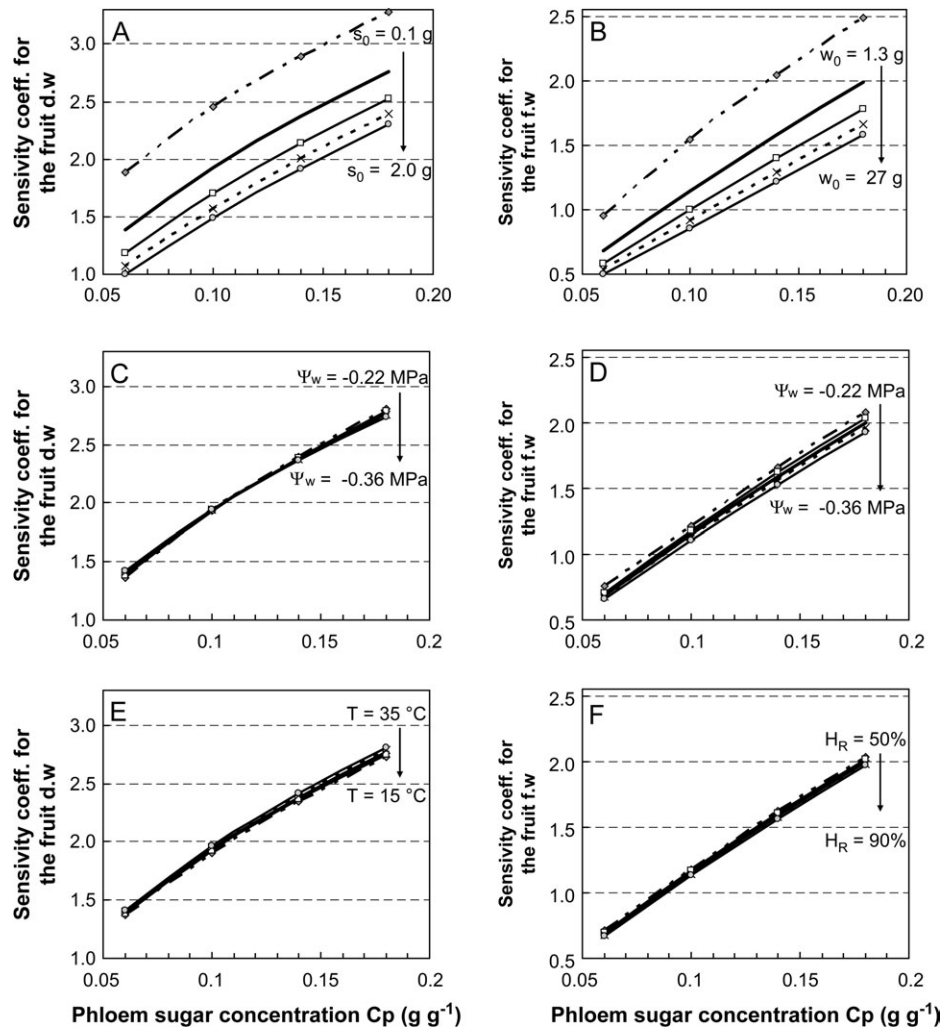
Fig. 6. Sensivity coefficients to the phloem sugar concentration (C_p) in interaction with the initial dry weight (A), initial fresh weight (B), stem water potential (C, D), air temperature (E), and humidity (F), calculated for the fruit dry weight (left graphs) and/or fresh weight (right graphs). Arrows indicate the range and course of variations from minimum to maximum values as indicated in Table 3.

Discussion

The need for ecophysiological models of fruit quality has recently been emphasized (Struik *et al*., 2005; Génard *et al*., 2007), as models are powerful tools to understand complex system behaviour and to point out key-processes and/or key developmental stages involved in the control of complex traits, such as quality. In horticulture, the Fishman and Génard (1998) model pioneered the modelling of fruit quality by combining carbon and water fluxes and allowing the prediction of both fruit size and dry matter content. Since its development on peach fruit, the generic character of this model has been evaluated on mango fruit with only minor modifications (Léchaudel *et al*., 2005, 2007) and it was also able to predict the intraspecies variability of peach growth in a heterogeneous population (Quilot *et al*., 2005*a, b*). The present adaptation

to tomato fruit confirmed the generic quality of the model and its suitability for fleshy berry fruit. Only a few modifications have been made, which have focused on three particular points in agreement with the literature on tomato: (i) the reflection coefficient (σ in equation 5) accounting for the cell wall permeability to sugars rose during fruit development representing a shift from symplasmic to apoplasmic transport of sugars. This shift had already appeared around 11 daa and apoplasmic unloading prevailed after 30 daa (Fig. 1A), in accordance with the literature (Ho, 2003*b*). (ii) The decrease of the cell wall extensibility during fruit growth. (iii) The inhibitor accumulation driving the decline of U_a (rate of active carbon uptake) depended on the initial fruit size (equation 6), whereas it was only developmentally controlled in the original model. According to the function described in equation 6, the maximum uptake of sucrose (V_{max}) was 0.0042 g g^{-1} DW h^{-1} at the

beginning of the simulation (t=10 daa) and 0.0017 g g^{-1} DW h^{-1} at maturity (t=60 daa) for the average initial fruit weight (Fig. 1B). Ruan *et al.* (1997) estimated the maximum hexose uptake rate (V_{max}) of 20–25 daa tomato fruit between 0.0054 and 0.0075 g g^{-1} DW h^{-1}.

On the whole, the model was able to simulate reasonably well several contrasting experimental situations with a common set of parameters. Moreover, despite a high sensitivity of the model to C_p (phloem concentration in sugar), a constant value could be applied to simulate the whole range of experimental data. The few situations in which the goodness-of-fit was reduced seemed to be mainly related to the inaccurate estimation of the initial fruit weight. For instance the 2F treatments were accurately predicted by the model at 25 °C and 20/25 °C but not at 20 °C (Fig. 3) for which the initial weight was quite low compared with the two other temperature treatments (Table 2). Although the mean sensitivity coefficient to s_0 or w_0 was moderate (0.25 and 0.39 for the dry and fresh weights, respectively; Fig. 5), a slight underestimation of s_0, for instance 0.25 g instead of 0.4 g, would lead to an underestimation of the final fruit fresh and dry weights of 63 g and 2.1 g, respectively. This range of underestimations is exactly that observed in case of the 20°C-2F treatment (Fig. 3B). As large variations in fruit size occur in the early period of fruit development in response to plant and environmental factors, the accurate estimation or measurement of the initial fruit weight appears as essential for the model initialization. This is confirmed in case of the two experimental datasets taking into account the fruit position (Fig. 4). In the case of the 2520°C-5F treatment, despite a global underestimation, the model predicted well the large differences between proximal and distal fruits only on the basis of different initial weights. In the case of the 2520°C-6F treatment, these differences were low (Table 2) as fruits were picked on the first truss of topped plants, that is in conditions of low competition among sinks.

In this study, the model could be used to analyse fruit functioning and to integrate the complex responses to plant or environmental factors. Under the standard situation defined in Table 3, the amount of water imported by the fruit via the phloem and xylem tissues peaked around 5 g d^{-1} fruit^{-1} and 0.5 g d^{-1} fruit^{-1}, respectively. These values are in the range of values reported in the literature for tomato fruit (Ho *et al.*, 1987; Plaut *et al.*, 2004; Guichard *et al.*, 2005). As reported by Ho *et al.* (1987) and Mitchell *et al.* (1991), the fruit osmotic pressure was relatively stable during fruit development, except in the case of carbon stress and the simulated fruit water potential was in the range of values reported by different authors (Johnson *et al.*, 1992; Guichard *et al.*, 2005). By contrast, fruit turgor was higher than that measured on cell or pericarp pieces, which remains under 0.3 MPa (Ehret and Ho, 1986*a*; Johnson *et al.*, 1992;

Grange, 1995; Thompson *et al.*, 1998) or around 0.4 MPa (S Guichard, unpublished data). However, Grange (1995) showed that growth rate of tomato pericarp slices is maximum for a turgor pressure around 0.4–0.5 MPa, which is the range of values predicted by the model for the period of rapid growth (Fig. 7). Moreover measurements of tissue turgor are currently performed on isolated cells or pericarp pieces without the dominant epidermis constraint (Thompson *et al.*, 1998), and thus they may underestimate the actual pressure. In the model, the fruit turgor integrates all the constraints as no tissue compartmentation is considered, and the increase in turgor pressure until ripening probably resulted from the decrease in cell/fruit plasticity induced by the drop of cell wall extensibility (Fig. 1A).

The analysis of the fruit functioning under virtual carbon or water stress situations (Fig. 7) outlined interesting reactions, thanks to interactions and feedback effects among the different fruit components which were difficult to anticipate beforehand. These unexpected properties generated by ecophysiological models are so-called emergent properties (Génard *et al.*, 2007) and they may be very informative for understanding and controlling fruit growth better. For instance any modification of the fruit osmotic pressure, related to low water or carbon input, influenced the xylem and phloem influx and thus the turgor pressure which, in turn, affected the growth. Compensating effects occurred, as for instance the increase of fruit osmotic potential at low air humidity, or the reduction of respiration and transpiration rates in case of low stem water potential. All applied stresses led to smaller fruits with large variations in dry matter concentration (+8% at low humidity, +27% at low stem water potential, and –41% at low phloem sugar concentration). These effects are consistent with experiments on water or salinity stresses or on factors reducing the leaf carbon supply (Ehret and Ho, 1986*b*; Ho, 2003*a*, b; Plaut *et al.*, 2004; Guichard *et al.*, 2005). Thus model may be used to perform virtual experiments and it should help in quantifying and optimizing the impact of fluctuating environment on fruit growth and dry matter concentration. It might also be easily applied to test virtual mutants affected on particular traits, for instance, on the transport of sugars, on the cuticular permeability to water, or on specific enzymes involved in the regulation of cell wall extensibility during fruit development.

Conclusion

The tomato model proposed in this work is based on simple biophysical laws and includes a relatively low number of parameters. It was able to mimic the fruit behaviour and to analyse the interactions and feedback regulations among the fruit system components, for
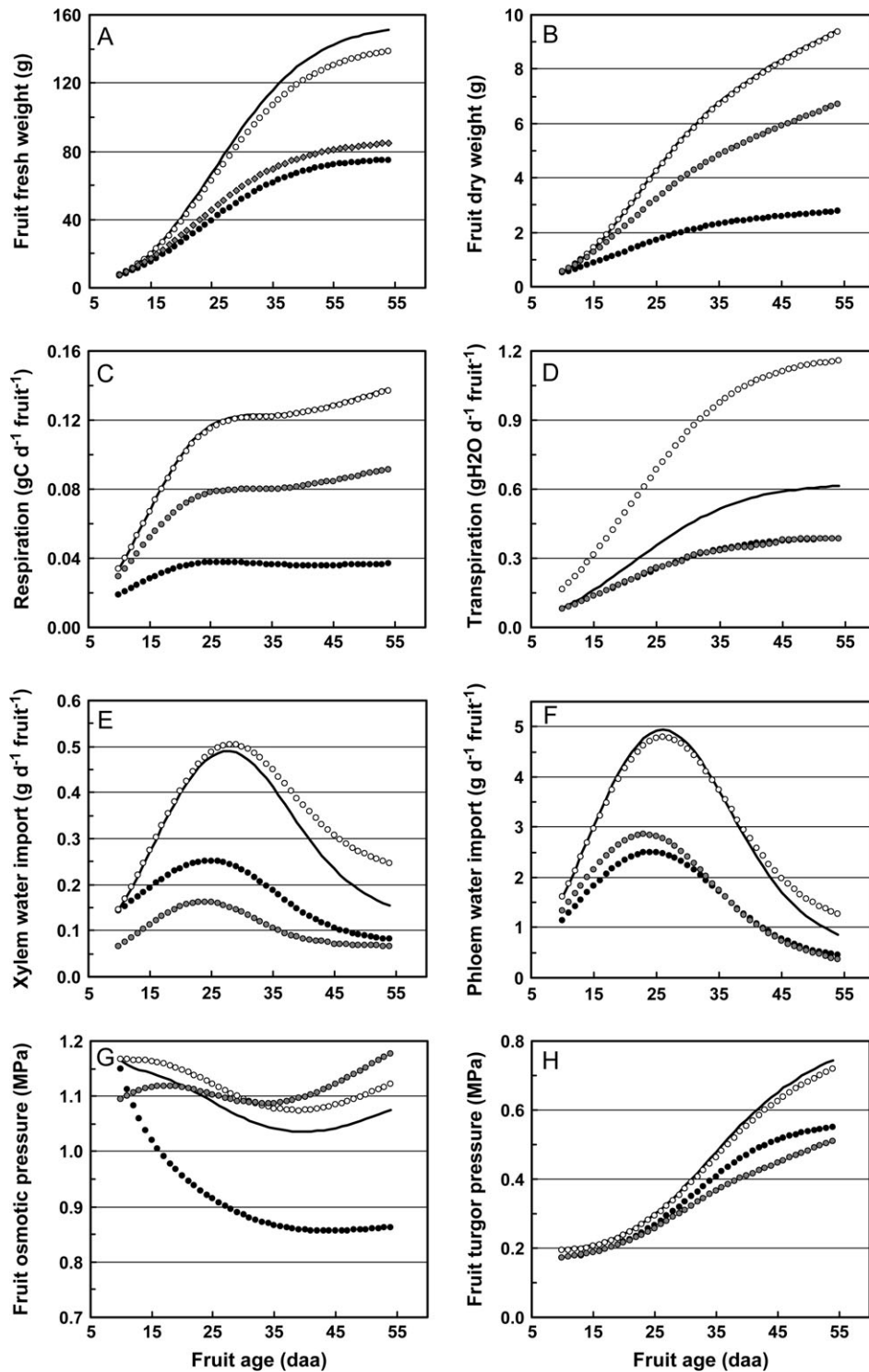
Fig. 7. Fruit growth, carbon and water fluxes, and osmotic and turgor pressures simulated under standard (bold lines), carbon stress (black circles), stem water potential stress (grey circles), and humidity stress (white circles). (A) Fruit fresh weight (g), (B) fruit dry weight (g), (C) respiration rate (g C d^{-1} fruit^{-1}), (D) transpiration rate (g H_2O d^{-1} fruit^{-1}), (E) xylem water import (g H_2O d^{-1} fruit^{-1}), (F) phloem water import (g H_2O d^{-1} fruit^{-1}), (G) fruit osmotic potential (MPa), and (H) fruit turgor pressure (MPa). Carbon stress was applied by reducing the phloem carbon concentration from 0.12 g g^{-1} to 0.06 g g^{-1}. Water stress was simulated by decreasing the stem water potential from – 0.22 MPa to – 0.6 MPa at constant air humidity (70%), and the air humidity stress corresponded to a drop from 70% to 40% at constant stem water potential (– 0.22 MPa).

instance, between fruit osmotic and turgor regulation and water and phloem fluxes in response to environmental and plant factors. Thus, it provides for scientists a tool to address genetic and agronomic questions concerning the control of quality and, in particular, the antagonism between size and composition.

Acknowledgements

References

Bargel H, Neinhuis C. 2005. Tomato (*Lycopersicon esculentum* Mill.) fruit growth and ripening as related to the biochemical properties of fruit skin and isolated cuticle. *Journal of Experimental Botany* **56,** 1049–1060.

Bertin N. 2005. Analysis of the tomato fruit growth response to temperature and plant fruit load in relation to cell division, cell expansion and DNA endoreduplication. *Annals of Botany* **95,** 439–447.

Bertin N, Borel C, Brunel B, Cheniclet C, Causse M. 2003*a*. Do genetic make-up and growth manipulation affect tomato fruit size by cell number, or cell size and DNA endoreduplication? *Annals of Botany* **92,** 415–424.

Bertin N, Bussières P, Génard M. 2006. Ecophysiological models of fruit quality: a challenge for peach and tomato. *Acta Hoticulturae* **718,** 633–641.

Bertin N, Fishman S, Génard M. 2003*b*. A model for early stage of tomato fruit development: cell multiplication and cessation of the cell proliferative activity. *Annals of Botany* **92,** 65–72.

Bertin N, Heuvelink E. 1993. Dry-matter production in a tomato crop: comparison of two simulation models. *Journal of Horticultural Science* **68,** 995–1011.

Brown MM, Hall JL, Ho LC. 1997. Sugar uptake by protoplasts isolated from tomato fruit tissues during various stages of fruit growth. *Physiologia Plantarum* **101,** 533–539.

Bussières P. 2002. Water import in the young tomato fruit limited by pedicel resistance and calyx transpiration. *Functional Plant Biology* **29,** 631–641.

Bussières P. 1994. Water import rate in tomato fruit: a resistance model. *Annals of Botany* **73,** 75–82.

Cosgrove DJ. 1985. Cell wall yield properties of growing tissue. *Plant Physiology* **78,** 347–356.

Cosgrove DJ. 1993. Wall extensibility: its nature, measurement and relationship to plant cell growth. *New Phytologist* **124,** 1–23.

Damon S, Hewitt J, Nieder M, Bennett AB. 1988. Sink metabolism in tomato fruit. *Plant Physiology* **87,** 731–736.

Ehret DL, Ho LC. 1986*a*. Effect of osmotic potential in nutrient solution on diurnal growth of tomato fruit. *Journal of Experimental Botany* **37,** 1294–1302.

Ehret DL, Ho LC. 1986*b*. Effect of salinity on dry matter partitioning and growth in tomato grown in nutrient film culture. *Journal of Horticultural Science* **61,** 361–367.

Fishman S, Génard M. 1998. A biophysical model of fruit growth: simulation of seasonal and diurnal dynamics of mass. *Plant, Cell and Environment* **21,** 739–752.

Gary C, Bot JL, Frossard JS, Andriolo JL. 1998. Ontogenetic changes in the construction cost of leaves, stems, fruit, and roots of tomato plants. *Journal of Experimental Botany* **49,** 59–68.

Génard M, Bertin N, Borel C, et al. 2007. Towards a virtual fruit focusing on quality: modelling features and potential uses. *Journal of Experimental Botany* **58,** 917–928.

Grange RI. 1995. Water relations and growth of tomato fruit pericarp tissue. *Plant, Cell and Environment* **18,** 1311–1318.

Guichard S, Bertin N, Leonardi C, Gary C. 2001. Tomato fruit quality in relation to water and carbon fluxes. *Agronomie* **21,** 385–392.

Guichard S, Gary C, Leonardi C, Bertin N. 2005. Analysis of growth and water relations of tomato fruits in relation to air vapor pressure deficit and plant fruit load. *Journal of Plant Growth Regulation* **24,** 201–213.

Heuvelink E, Bertin N. 1994. Dry matter partitioning in a tomato crop: comparison of two simulation models. *Journal of Horticultural Science* **69,** 885–903.

Ho LC. 2003*a*. Improving tomato fruit quality by cultivation. In: Cockshull KE, Gray D, Seymour GB, Thomas B, eds. *Genetic and environmental manipulation of horticultural crops*. UK: CABI Publishing, 17–29.

Ho LC. 2003*b*. Genetic and cultivation manipulation for improving tomato fruit quality. *Acta Horticulturae* **613,** 21–31.

Ho LC, Adams P. 1994. The physiological basis for high fruit yield and susceptibility to calcium deficiency in tomato and cucumber. *Journal of Horticultural Science* **69,** 367–376.

Ho LC, Grange RI, Picken AJ. 1987. An analysis of the accumulation of water and dry matter in tomato fruit. *Plant, Cell and Environment* **10,** 157–162.

Ho LC, Hewitt JD. 1986. Fruit development. In: Atherton JG, Rudich J, eds. *The tomato crop*. UK: Chapman and Hall, 201–240.

Johnson RW, Dixon MA, Lee DR. 1992. Water relations of tomato during fruit growth. *Plant, Cell and Environment* **15,** 947–953.

Kobayashi K, Us Salam M. 2000. Comparing simulated and measured values using mean squared deviation and its component. *Agronomy Journal* **92,** 345–352.

Léchaudel M, Génard M, Lescourret F, Urban L, Jannoyer M. 2005. Modelling effects of weather and source–sink relationships on mango fruit growth. *Tree Physiology* **25,** 583–597.

Léchaudel M, Vercambre G, Lescourret F, Normand F, Génard M. 2007. An analysis of elastic and plastic fruit growth of mango in response to various assimilate supplies. *Tree Physiology* **27,** 219–230.

Leonardi C, Baille A, Guichard S. 1999. Effects of fruit characteristics and climatic conditions on tomato transpiration in greenhouses. *Journal of Horticultural Science and Biotechnology* **74,** 748–756.

Lescourret F, Génard M. 2005. A virtual peach fruit model simulating changes in fruit quality during the final stage of fruit growth. *Tree Physiology* **25,** 1–13.

Lockhart JA. 1965. An analysis of irreversible plant cell elongation. *Journal of Theoretical Biology* **8,** 264–275.

Maggio A, Joly RJ. 1995. Effects of mercuric chloride on the hydraulic conductivity of tomato root systems, evidence for a channel-mediated water pathway. *Plant Physiology* **109,** 331–335.

Milner ID, Ho LC, Hall JL. 1995. Properties of proton and sugar transport at tonoplast of tomato (*Lycopersicon esculentum*) fruit. *Physiologia Plantarum* **94,** 399–410.

Mitchell JP, Shennan C, Grattan SR. 1991. Developmental changes in tomato fruit composition in response to water deficit and salinity. *Physiologia Plantarum* **83,** 177–185.

Nguyen-Quoc B, Foyer CH. 2001. A role for « futile cycles » involving invertase and sucrose synthase in sucrose metabolism of tomato fruit. *Journal of Experimental Botany* **52,** 881–889.

Nobel PS. 1974. *Introduction to biophysical plant physiology*. San Francisco, CA: W.H. Freeman and company.

Plaut Z, Grava A, Yehezkel C, Matan E. 2004. How do salinity and water stress affect transport of water, assimilates and ions to tomato fruit? *Physiologia Plantarum* **122,** 429–442.

Quilot B, Génard M, Lescourret F, Kervella J. 2005*a*. Simulating genotypic variation of fruit quality in an advanced peach×*Prunus davidiana* cross. *Journal of Experimental Botany* **56,** 3071–3081.

Quilot B, Kervella J, Génard M, Lescourret F. 2005*b*. Analysing the genetic control of peach fruit quality through an ecophysiological model combined with a QTL approach. *Journal of Experimental Botany* **56,** 3083–3092.

R Development Core Team. 2005. *R: A language and environment for statistical computing*. Vienna: R Foundation for Statistical Computing, 2005.

Ruan YL, Patrick JW. 1995. The cellular pathway of postphloem sugar transport in developing tomato fruit. *Planta* **196,** 434–444.

Ruan YL, Patrick JW, Brady C. 1997. Protoplast hexose carrier activity is a determinate of genotypic difference in hexose storage in tomato fruit. *Plant, Cell and Environment* **20,** 341–349.

Struik PC, Yin X, de Visser P. 2005. Complex quality traits: now time to model. *Trends in Plant Science* **10,** 513–516.

Thompson DS. 2001. Extensiometric determination of the rheological properties of the epidermis of growing tomato fruit. *Journal of Experimental Botany* **52,** 1291–1301.

Thompson DS, Davies WJ, Ho LC. 1998. Regulation of tomato fruit growth by epidermal cell wall enzymes. *Plant, Cell and Environment* **21,** 589–599.

Thorp KR, Batchelor WD, Paz JO. 2005. *A cross validation approach to evaluate CERES- Maize simulations of corn yield spatial variability*. ASAE Annual Meeting paper number 053002.

Zhang XY, Wang XL, Wang XF, Xia GH, Pan QH, Fan RC, Wu FQ, Yu XC, Zhang DP. 2006. A shift of phloem unloading from symplasmic to apoplasmic pathway is involved in developmental onset of ripening in grape berry. *Plant Physiology* **142,** 220–232.

Zonia L, Munnik T. 2007. Life under pressure: hydrostatic pressure in cell growth and function. *Trends in Plant Science* **12,** 90–97.

Zwieniecki MA, Boersma L. 1997. A technique to measure root tip hydraulic conductivity and root water potential simultaneously. *Journal of Experimental Botany* **48,** 333–336.